Chemical Science

ROYAL SOCIETY OF CHEMISTRY

EDGE ARTICLE

View Article Online
View Journal | View Issue

Cite this: *Chem. Sci.*, 2023, **14**, 2640

All publication charges for this article have been paid for by the Royal Society of Chemistry

Pressure-induced room-temperature phosphorescence enhancement based on purely organic molecules with a folded geometry†

Zhiqiang Yang, ‡[a] Zhiyuan Fu,‡[b] Haichao Liu, *[a] Min Wu,[b] Nan Li,[b] Kai Wang, *[b] Shi-Tong Zhang,[a] Bo Zou *[b] and Bing Yang *[a]

Received 11th January 2023
Accepted 7th February 2023

DOI: 10.1039/d3sc00172e

rsc.li/chemical-science

The pressure-dependent luminescence behavior of purely organic compounds is an important topic in the field of stimulus-responsive smart materials. However, the relevant studies are mainly limited to the investigation of fluorescence properties, while room-temperature phosphorescence (RTP) of purely organic compounds has not been investigated. Here, we filled in this gap regarding pressure-dependent RTP by using a model molecule selenanthrene (SeAN) with a folded geometry. For the first time to the best of our knowledge, a unique phenomenon involving pressure-induced RTP enhancement was discovered in an SeAN crystal, and an underlying mechanism involving folding-induced spin–orbit coupling enhancement was revealed. Pressure-induced RTP enhancement was also observed in an analog of SeAN also showing a folded geometry, but in this case yielded a white-light emission that is very rare in purely organic RTP-displaying materials.

Stimulus-responsive smart materials are attracting increasing attention due to their diverse functions and wide applications. With the development of material science, ever more external stimuli such as light,[1–5] heat,[6–8] pressure,[9–11] gas,[12,13] and moisture[14,15] can be sensed and detected in which some sensing materials respond to external pressure stimulation through a change in luminescence. For example, piezochromic luminescent materials can change their colors in response to changes in external pressure, a feature allowing for a real-time visual imaging of pressure response.[16,17] However, to date, most piezochromic luminescent materials have been mainly limited to fluorescence systems,[18,19] and there have been very few related studies on room-temperature phosphorescence (RTP).[20,21]

Usually, RTP can be produced, albeit inefficiently, from triplet excitons in purely organic materials, and the effective utilization of triplet excitons has been studied systematically in organic light-emitting diodes.[22–25] From the perspective of structure–property relationship, pressure may be an important external factor that affects the generation of RTP and regulates its properties. There are only a handful of reports on piezochromic RTP of metal complexes,[26,27] and apparently none on piezochromism of purely organic RTP-displaying materials. This absence of reports may be a consequence of purely organic RTP-displaying materials being difficult to obtain due to their weak spin–orbit coupling (SOC).[28,29] Also, even though efficient RTP has been achieved in purely organic materials,[30–34] it may coexist and even merge with its counterpart fluorescence, which makes it difficult to analyze RTP piezochromism. Therefore, to study the piezochromic behavior of RTP, a purely organic model molecule displaying only RTP emission is highly desirable in order to exclude interference by fluorescence.

Previously, we proposed a mechanism of folding-induced enhancement of SOC for thianthrene (TA) crystals displaying efficient RTP.[35,36] SOC coefficients of TA with a folded geometry can be improved by several orders of magnitude relative to those of a planar conformation. Using this strategy, a series of TA derivatives with a dual emission, namely fluorescence and RTP, have been developed.[12,13] However, these materials are not suitable for the study of pressure-dependent RTP behavior due to the fluorescence interference. The recent successful application of selenium (Se)-containing RTP materials in organic light-emitting diodes[37,38] has inspired us to search for materials displaying only RTP. In the current work, an analogue of TA, namely selenanthrene (SeAN), was chosen as a model molecule, in which the S atoms in TA were replaced with Se atoms in order to introduce a heavy-atom effect while maintaining the folded geometry (Fig. 1a and b). As expected, the produced SeAN crystals exhibited RTP-only emission, *i.e.*, with almost no

[a]*State Key Laboratory of Supramolecular Structure and Materials, College of Chemistry, Jilin University, Changchun 130012, China. E-mail: hcliu@jlu.edu.cn; yangbing@jlu.edu.cn*

[b]*State Key Laboratory of Superhard Materials, College of Physics, Jilin University, Changchun 130012, China. E-mail: kaiwang@jlu.edu.cn; zoubo@jlu.edu.cn*

† Electronic supplementary information (ESI) available. CCDC 2213389. For ESI and crystallographic data in CIF or other electronic format see DOI: https://doi.org/10.1039/d3sc00172e

‡ These authors contributed equally.

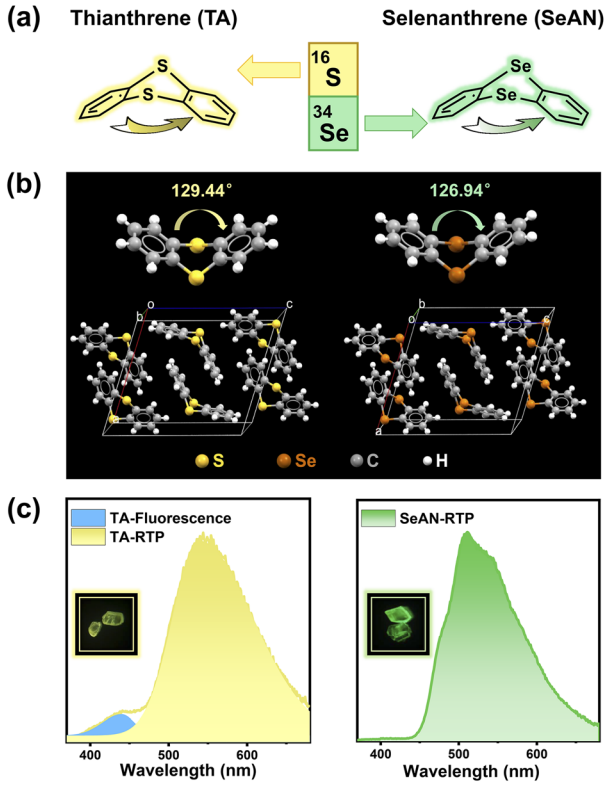

Fig. 1 (a) Molecular structures of TA and SeAN. (b) Molecular configuration and packing characteristics in crystals. (c) Emission properties of TA and SeAN single crystals under ambient conditions.

coexisting fluorescence. With the aid of a diamond anvil cell (DAC),[39,40] we discovered a special pressure-induced RTP enhancement in the purely organic SeAN crystal, which has never been reported before to the best of our knowledge. Experimental and theoretical investigations revealed that this pressure-induced RTP enhancement can be ascribed to an improved triplet radiative transition rate, in turn due to a strengthened SOC resulting from a more folded geometry, together with the suppression of nonradiative molecular motions resulting from enhanced intermolecular interactions under high pressure. The TA crystal also showed pressure-induced enhancement of RTP, specifically an interesting pressure-induced white-light emission.

First, SOC coefficients of both TA and SeAN were calculated as a function of folding dihedral angle[41] (Fig. S1a and b†). The calculations demonstrated TA and SeAN both being subjected to the same overall effect of folding-induced SOC enhancement, *i.e.*, the SOC coefficients of the molecules with a folded geometry were several orders of magnitude better than those with a planar conformation. But at any given dihedral angle, the SOC coefficient of SeAN was 5–6 times higher than that of TA. For SeAN, a cooperative effect between the folded conformation of the molecular skeleton and heavy-atom effect of Se atoms was expected to result in a greatly accelerated intersystem crossing (ISC), and hence an RTP-only emission. Then, SeAN was synthesized according to a one-step reaction process (Scheme S1†). Compared with the bright blue emission of TA in a solution with a photoluminescence quantum yield (PLQY) of 1.74%,[35] we did not detect any luminescence signal from a dilute solution of SeAN. The non-luminescence of SeAN in dilute solution can be attributed to its poor singlet radiative ability as well as reduced singlet exciton population due to the enhanced SOC accelerating ISC competition for populating triplet excitons; however, these mass-produced triplet excitons would be seriously deactivated by nonradiative motions of SeAN molecules. At low temperature (77 K), SeAN exhibited bright blue-green emission with a peak at a wavelength of 447 nm (Fig. S2†), whereas TA showed a dual emission, namely a weak fluorescence (436 nm) and dominant phosphorescence (486 nm).[36] More importantly, colorless block crystals of SeAN were obtained by performing sublimation. Just like TA in its crystal, SeAN showed a folded molecular geometry with a dihedral angle of 126.94°, and with SeAN molecules stacked in a form of dimers with an interplanar π–π separation of 3.525 Å (Fig. 1b and S3a†). The SeAN crystals exhibited only a vibronic-structured RTP emission band as highly desired, with a maximum intensity at a wavelength of 510 nm and a lifetime of 6.92 ms, while the TA crystals showed a dual emission, *i.e.*, fluorescence and RTP (Fig. S3b and c†). The SeAN crystals showed a PLQY of 4.80% and an emerald color, with this color resulting from nearly pure RTP (Fig. 1c). Based on the well-defined packing structure and unique RTP-only emission of SeAN, we were able to observe the pressure-dependent behavior of RTP from a purely organic compound and reveal the intrinsic structure–property relationship.

Next, isotropic hydrostatic pressure produced by use of a DAC[39,40] was applied to the SeAN crystal. With increasing pressure, the absorption of light by the SeAN crystal showed a continuous redshift (Fig. S4†), whereas the emission exhibited a distinct two-stage change. At the first stage, as the pressure was increased from 1 atm to 4.15 GPa, the RTP emission of the SeAN crystal gradually increased in intensity, accompanied by

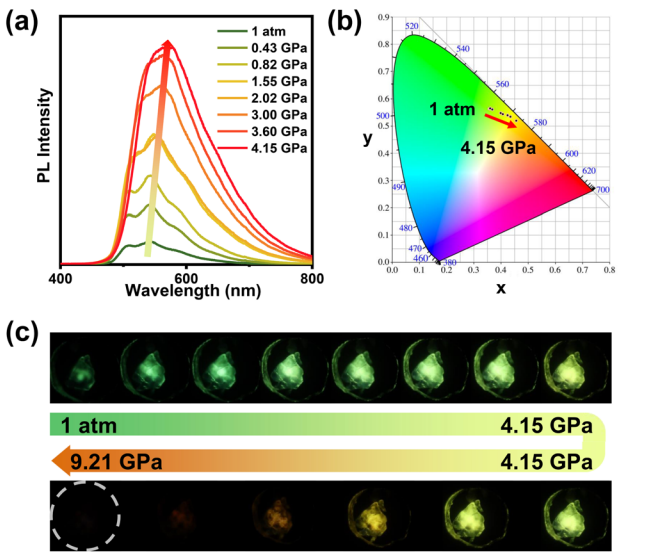

Fig. 2 (a) Emission spectra, (b) CIE coordinates, and (c) luminescence photographs of a SeAN single crystal under different pressures.

a small redshift from green to yellow-green (Fig. 2). The vibronic structure of the emission spectrum gradually disappeared, with a single peak at 567 nm observed when the pressure reached 4.15 GPa. The emission intensity at 4.15 GPa was enhanced by a factor of 9.49 compared to that at 1 atm. This pressure-induced RTP enhancement was an attractive case of skillfully combining use of purely organic RTP-displaying material with application of high pressure. At the second stage, when the pressure was further increased beyond 4.15 GPa, the RTP emission of the SeAN crystal showed a sharp decrease in intensity along with a significant redshift from yellow-green to orange-red, and finally became completely quenched when the pressure reached 9.21 GPa (Fig. 2c and S5†). The luminescence quenching may have been caused by greatly enhanced π–π interactions,[9,42] consistent with the case of the fluorescence system under application of pressure.[43–46] During the decompression, emission spectra showed a reversible change in intensity and shape (Fig. S6†).

To understand the mechanism of the pressure-induced RTP enhancement presented above, high-pressure angle-dispersive X-ray diffraction (ADXRD) tests were performed on the SeAN crystals. During the pressurization, neither diffraction peak disappeared nor did any new diffraction peak form, and the characteristic diffraction peaks all shifted to high angles (Fig. 3a), which can exclude the possibility of a phase transition. After the pressure was released, the diffraction pattern reverted essentially exactly to that of the initial state, which indicated a reversible recovery of the crystal structure (Fig. S7†). This structural reversibility corresponded to the reversible emission spectrum. Inspection of the crystal structure showed an intermolecular π–π dimer loosely packed mainly along the *c*-axis of unit cell; and therefore, the crystal may be more easily compressed in this direction due to little steric hindrance, as confirmed by the high-pressure ADXRD tests (Fig. 3a, b and S8a†).[9]

Theoretical simulations on the crystal structures were performed to understand the changes in the molecular geometry and crystal packing motif under applications of different pressures. During compression, the π···π distance in the SeAN dimers was reduced prominently, accompanied by a decrease in the folding dihedral angle of the SeAN molecules (Fig. 3c and S8b†). Through Hirshfeld surface analysis, interactions between SeAN molecules were determined to have become gradually enhanced as the molecules got closer to each other with increasing pressure (Fig. S9†). The contribution of the C···C interaction to the Hirshfeld surface increased from 3.7% to 4.3%, while that of the C···H interaction increased from 20.4% to 21.5% (Fig. S10†). These results indicated that, as would generally be expected, more intermolecular interactions occurred as the pressure was increased, which surely contributed to the restriction of molecular motions and effective suppression of non-radiative quenching of triplet excitons.

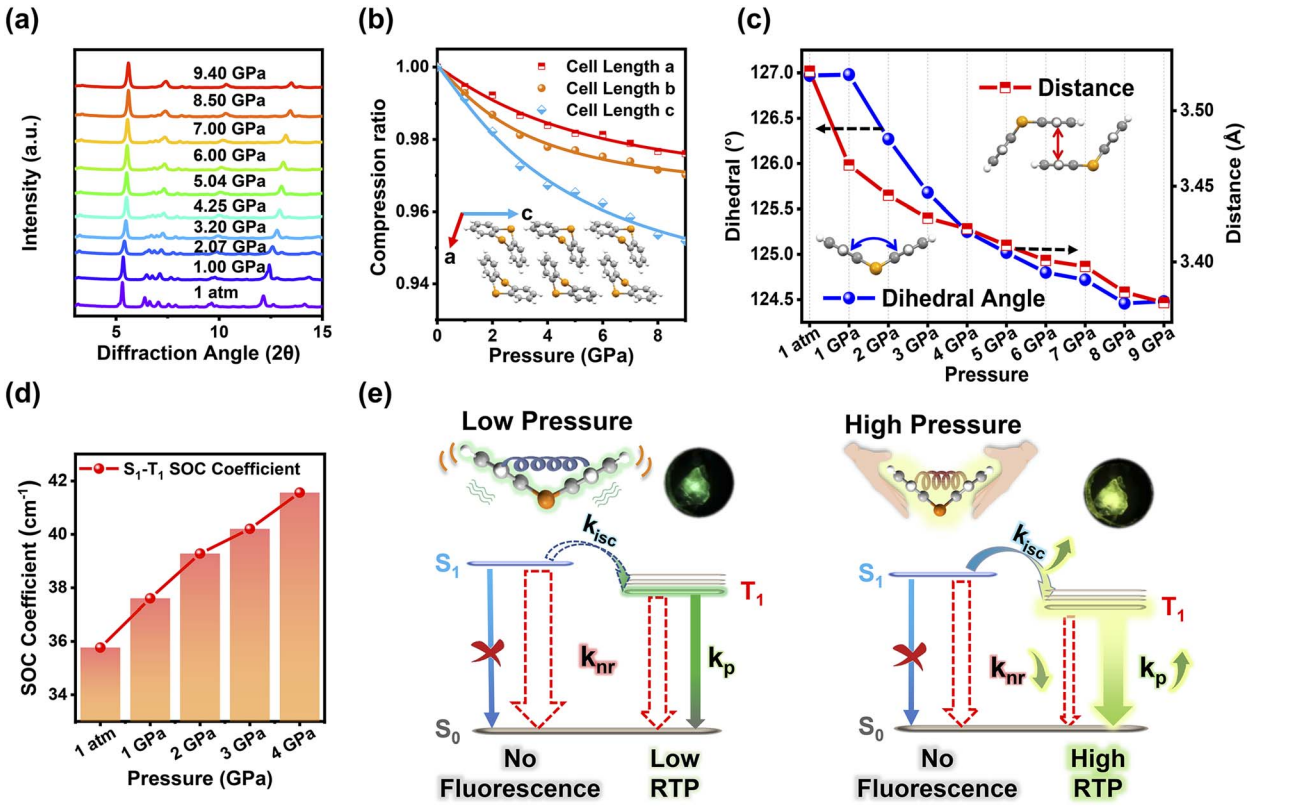

Fig. 3 (a) ADXRD patterns, (b) compression ratios of each crystal axis obtained using Pawley refinement, and (c) extents of folding of SeAN in its crystal under different pressures. (d) S_1–T_1 SOC coefficients of an SeAN monomer under different pressures. (e) Schematic illustration of the pressure-induced enhancement of the RTP of the SeAN crystal.

Furthermore, based on the crystal structures of SeAN under different pressures, theoretical calculations of SOC coefficients were carried out on a single SeAN molecule to comprehensively understand the nature of the pressure-induced RTP enhancement. SOC has been shown to be a key factor determining whether or not RTP emission from a purely organic material occurs, and therefore SOC coefficients between singlet and triplet states under different pressures were primarily considered in our work (Fig. 3d). The SOC coefficient between S_1 and T_1 increased steadily with increasing pressure from 1 atm to 4 GPa. This increase was mainly ascribed to a decrease in the folding dihedral angle of the SeAN molecule with increasing pressure, and was also in accord with the results obtained from theoretical calculations of the SOC coefficient as a function of folding dihedral angle (Fig. S1†). In addition, most of the SOC coefficients between high-lying T_n and S_1 states were shown to be increased, albeit to different degrees, at 4 GPa compared to those at 1 atm (Fig. S11–S13†).[47] An enhanced SOC was apparently conducive to the ISC process, specifically to increasing the triplet exciton population in the SeAN crystal under high pressure. Regarding the triplet radiative transition, as the pressure was increased, RTP lifetime gradually decreased and PLQY greatly improved, which demonstrated the increase in triplet radiative transition rate under high pressure (Fig. S14 and Table S1†). To verify the rationality of the model on a single-molecule level, theoretical calculations on the SeAN dimer were also performed. However, based on the electron–hole pair wavefunction of S_1 and T_1 states,[48] no charge-transfer interaction between two molecules in the SeAN dimer was indicated (Fig. S15†). Like the case for the monomer, the SOC coefficient between S_1 and T_1 of the SeAN dimer tended to increase as the external pressure was increased (Fig. S16†). These results taken together indicated a predominant role of the monomers in the photophysical behavior of the SeAN crystals under different pressures. The folded molecular geometry of the SeAN molecule was revealed, according to analysis of natural transition orbitals (NTOs), to promote a change in transition configuration of the S_1 state (from $^1(\pi, \pi^*)$ to $^1(n, \pi^*)$ and $^1(n, \sigma^*)$), but to not affect $^3(\pi, \pi^*)$ of the T_1 state. Different transition configurations between S_1 and T_1 states were indicated to be favorable for promoting the ISC process according to the El-Sayed rule (Fig. S17†).[49] This result was noted to be consistent with a systematic study of TA in our previous works, and further demonstrated the generality of folding-induced SOC enhancement.[35,36] As a result, we could attribute the pressure-induced enhancement of RTP of SeAN crystals to (1) an increased degree of folding of the SeAN molecule under high pressure giving rise to enhanced SOC and accelerated ISC, a feature increasing the triplet exciton population, and (2) the high-pressure environment effectively improving the radiative transition rate of triplet excitons due to enhanced SOC and suppressing the non-radiative quenching (Fig. 3e).

To verify the universality of the pressure-induced RTP enhancement, the RTP response of a TA sample to pressure was also investigated. As expected, the powder crystals of TA exhibited the pressure-induced RTP enhancement, like that observed for the SeAN crystals. But the powder crystals of TA also showed a pressure-induced fluorescence enhancement. This fluorescence enhancement may have been due to the suppression of nonradiative molecular motions having been more prevalent than the improvement of the ISC process – with the composite effect of these two factors decreasing the nonradiative transition rate, and hence finally resulting in the fluorescence enhancement. As a whole, the simultaneous enhancement of both RTP emission and fluorescence emission with increasing pressure was observed to give rise to a change in emission color from yellow to white (Fig. 4 and S18†). Such pressure-induced white-light emission is very rare, especially for purely organic materials,[10] hence demonstrating the fundamental and potentially practical importance of such materials. And the utilization of RTP from purely organic materials charts a new course for realizing piezochromic luminescence with enhanced emission and rich color.

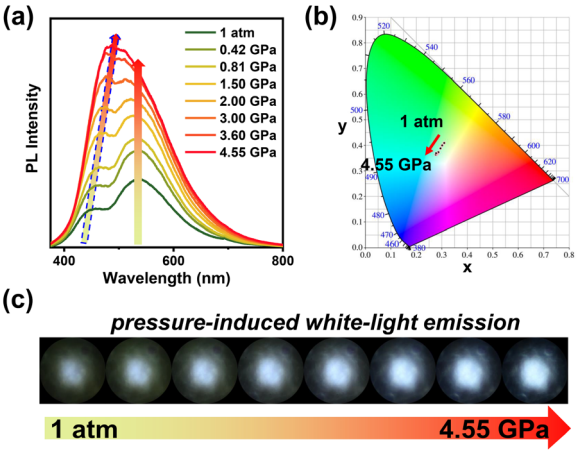

Fig. 4 (a) Emission spectra, (b) CIE coordinates, and (c) luminescence photographs of TA powder crystals under different pressures.

Conclusions

In summary, the synergy of folding-induced SOC enhancement and the heavy-atom effect was found to result in RTP-only emission of SeAN crystals. The concise structure of SeAN crystals made it possible for us to investigate in depth the pressure-dependent behavior of RTP from a purely organic material and reveal its mechanism. An unprecedented phenomenon involving pressure-induced enhancement of RTP from a purely organic material was discovered for SeAN crystals, and can be mainly ascribed to enhanced SOC, improved triplet radiative transition rate, and suppressed nonradiative decay under high pressure. This property was found to be well inherited by the TA crystals, and thereby a rare pressure-induced emission of white light was achieved. This work – having shown a phenomenon of pressure-induced RTP enhancement and its underlying mechanism – has provided a new approach, involving application of high pressure, for promoting the production of RTP from a purely organic material and the regulation of its properties. This work has also provided a better understanding of the origin of triplet excitons and the nature of triplet aggregates.

Data availability

All necessary information is included in the ESI.†

Author contributions

Conceptualization: H. L., K. W., S.-T. Z. and B. Y. Data curation: Z. Y., Z. F., M. W. and N. L. Chemical synthesis and product analysis: Z. Y. DFT calculations: Z. Y. and Z. F. Supervision: H. L., K. W., B. Z. and B. Y. Funding acquisition: H. L. and B. Y. Writing – original draft: Z. Y. Writing – review & editing: H. L., K. W., B. Z. and B. Y.

Conflicts of interest

There are no conflicts to declare.

Acknowledgements

This work is supported by the National Natural Science Foundation of China (No. 51873077, 52103209, and 52073117) and the National Key Research and Development Program of China (No. 2020YFA0714603). ADXRD experiments were performed at the BL15U1 beamline, Shanghai Synchrotron Radiation Facility (SSRF). We also thank HZWTECH for providing computation facilities for this study.

Notes and references

1 A. H. Gelebart, D. Jan Mulder, M. Varga, A. Konya, G. Vantomme, E. W. Meijer, R. L. B. Selinger and D. J. Broer, *Nature*, 2017, **546**, 632–636.
2 Y. Zhang, L. Gao, X. Zheng, Z. Wang, C. Yang, H. Tang, L. Qu, Y. Li and Y. Zhao, *Nat. Commun.*, 2021, **12**, 2297.
3 J. Yang, M. Fang and Z. Li, *InfoMat*, 2020, **2**, 791–806.
4 Y. Li, F. Gu, B. Ding, L. Zou and X. Ma, *Sci. China: Chem.*, 2021, **64**, 1297–1301.
5 L. Gu, H. Wu, H. Ma, W. Ye, W. Jia, H. Wang, H. Chen, N. Zhang, D. Wang, C. Qian, Z. An, W. Huang and Y. Zhao, *Nat. Commun.*, 2020, **11**, 944.
6 J. Du, L. Sheng, Y. Xu, Q. Chen, C. Gu, M. Li and S. X. Zhang, *Adv. Mater.*, 2021, **33**, e2008055.
7 D. Li, J. Yang, M. Fang, B. Z. Tang and Z. Li, *Sci. Adv.*, 2022, **8**, eabl8392.
8 J. Chen, N. U. Rahman, Z. Mao, J. Zhao, Z. Yang, S. Liu, Y. Zhang and Z. Chi, *J. Mater. Chem. C*, 2019, **7**, 8250–8254.
9 H. Liu, Y. Gu, Y. Dai, K. Wang, S. Zhang, G. Chen, B. Zou and B. Yang, *J. Am. Chem. Soc.*, 2020, **142**, 1153–1158.
10 R. Fu, W. Zhao, L. Wang, Z. Ma, G. Xiao and B. Zou, *Angew. Chem., Int. Ed.*, 2021, **60**, 10082–10088.
11 J. Ren, Y. Wang, Y. Tian, Z. Liu, X. Xiao, J. Yang, M. Fang and Z. Li, *Angew. Chem., Int. Ed.*, 2021, **60**, 12335–12340.
12 H. Liu, G. Pan, Z. Yang, Y. Wen, X. Zhang, S.-T. Zhang, W. Li and B. Yang, *Adv. Opt. Mater.*, 2022, **10**, 2102814.
13 Z. Yang, S. Zhao, X. Zhang, M. Liu, H. Liu and B. Yang, *Front. Chem.*, 2021, **9**, 810304.
14 H. Gui, Z. Huang, Z. Yuan and X. Ma, *CCS Chem.*, 2022, **4**, 173–181.
15 T. Zhang, Y. Wu and X. Ma, *Chem. Eng. J.*, 2021, **412**, 128689.
16 Y. Fang, L. Zhang, Y. Yu, X. Yang, K. Wang and B. Zou, *CCS Chem.*, 2021, **3**, 2203–2210.
17 Z. Ma, F. Li, D. Zhao, G. Xiao and B. Zou, *CCS Chem.*, 2020, **2**, 71–80.
18 Q. Sui, X.-T. Ren, Y.-X. Dai, K. Wang, W.-T. Li, T. Gong, J.-J. Fang, B. Zou, E.-Q. Gao and L. Wang, *Chem. Sci.*, 2017, **8**, 2758–2768.
19 S. Wan, Z. Ma, C. Chen, F. Li, F. Wang, X. Jia, W. Yang and M. Yin, *Adv. Funct. Mater.*, 2016, **26**, 353–364.
20 A. Li, S. Xu, C. Bi, Y. Geng, H. Cui and W. Xu, *Mater. Chem. Front.*, 2021, **5**, 2588–2606.
21 Y. Wang, J. Yang, M. Fang, Y. Yu, B. Zou, L. Wang, Y. Tian, J. Cheng, B. Z. Tang and Z. Li, *Matter*, 2020, **3**, 449–463.
22 H. Uoyama, K. Goushi, K. Shizu, H. Nomura and C. Adachi, *Nature*, 2012, **492**, 234–238.
23 C.-J. Chiang, A. Kimyonok, M. K. Etherington, G. C. Griffiths, V. Jankus, F. Turksoy and A. P. Monkman, *Adv. Funct. Mater.*, 2013, **23**, 739–746.
24 L. Yao, S. Zhang, R. Wang, W. Li, F. Shen, B. Yang and Y. Ma, *Angew. Chem., Int. Ed.*, 2014, **53**, 2119–2123.
25 X. Chen, D. Ma, T. Liu, Z. Chen, Z. Yang, J. Zhao, Z. Yang, Y. Zhang and Z. Chi, *CCS Chem.*, 2022, **4**, 1284–1294.
26 Y. Ai, Y. Li, M. H. Chan, G. Xiao, B. Zou and V. W. Yam, *J. Am. Chem. Soc.*, 2021, **143**, 10659–10667.
27 M. Xie, X. R. Chen, K. Wu, Z. Lu, K. Wang, N. Li, R. J. Wei, S. Z. Zhan, G. H. Ning, B. Zou and D. Li, *Chem. Sci.*, 2021, **12**, 4425–4431.
28 Z. Yang, C. Xu, W. Li, Z. Mao, X. Ge, Q. Huang, H. Deng, J. Zhao, F. L. Gu, Y. Zhang and Z. Chi, *Angew. Chem., Int. Ed.*, 2020, **59**, 17451–17455.
29 W. Zhao, Z. He and B. Z. Tang, *Nat. Rev. Mater.*, 2020, **5**, 869–885.
30 Y. Wen, H. Liu, S. Zhang, J. Cao, J. De and B. Yang, *Adv. Opt. Mater.*, 2020, **8**, 1901995.
31 X. Ma, C. Xu, J. Wang and H. Tian, *Angew. Chem., Int. Ed.*, 2018, **57**, 10854–10858.
32 Z. Yin, M. Gu, H. Ma, X. Jiang, J. Zhi, Y. Wang, H. Yang, W. Zhu and Z. An, *Angew. Chem., Int. Ed.*, 2021, **60**, 2058–2063.
33 Y. Wen, H. Liu, S.-T. Zhang, G. Pan, Z. Yang, T. Lu, B. Li, J. Cao and B. Yang, *CCS Chem.*, 2021, **3**, 1940–1948.
34 J. Wang, X. Yao, Y. Liu, H. Zhou, W. Chen, G. Sun, J. Su, X. Ma and H. Tian, *Adv. Opt. Mater.*, 2018, **6**, 1800074.
35 H. Liu, Y. Gao, J. Cao, T. Li, Y. Wen, Y. Ge, L. Zhang, G. Pan, T. Zhou and B. Yang, *Mater. Chem. Front.*, 2018, **2**, 1853–1858.
36 G. Pan, Z. Yang, H. Liu, Y. Wen, X. Zhang, Y. Shen, C. Zhou, S.-T. Zhang and B. Yang, *J. Phys. Chem. Lett.*, 2022, **13**, 1563–1570.
37 D. R. Lee, K. H. Lee, W. Shao, C. L. Kim, J. Kim and J. Y. Lee, *Chem. Mater.*, 2020, **32**, 2583–2592.
38 C. L. Kim, J. Jeong, D. R. Lee, H. J. Jang, S.-T. Kim, M.-H. Baik and J. Y. Lee, *J. Phys. Chem. Lett.*, 2020, **11**, 5591–5600.
39 P. F. McMillan, *Chem. Commun.*, 2003, 919–923.

40 H.-K. Mao, X.-J. Chen, Y. Ding, B. Li and L. Wang, *Rev. Mod. Phys.*, 2018, **90**, 015007.
41 Y. Zhang, B. Suo, Z. Wang, N. Zhang, Z. Li, Y. Lei, W. Zou, J. Gao, D. Peng, Z. Pu, Y. Xiao, Q. Sun, F. Wang, Y. Ma, X. Wang, Y. Guo and W. Liu, *J. Chem. Phys.*, 2020, **152**, 064113.
42 H. Liu, Y. Dai, Y. Gao, H. Gao, L. Yao, S. Zhang, Z. Xie, K. Wang, B. Zou, B. Yang and Y. Ma, *Adv. Opt. Mater.*, 2018, **6**, 1800085.
43 S. Zhang, Y. Dai, S. Luo, Y. Gao, N. Gao, K. Wang, B. Zou, B. Yang and Y. Ma, *Adv. Funct. Mater.*, 2017, **27**, 1602276.
44 H. Yuan, K. Wang, K. Yang, B. Liu and B. Zou, *J. Phys. Chem. Lett.*, 2014, **5**, 2968–2973.
45 Y. Liu, Q. Zeng, B. Zou, Y. Liu, B. Xu and W. Tian, *Angew. Chem., Int. Ed.*, 2018, **57**, 15670–15674.
46 J. Wu, Y. Cheng, J. Lan, D. Wu, S. Qian, L. Yan, Z. He, X. Li, K. Wang, B. Zou and J. You, *J. Am. Chem. Soc.*, 2016, **138**, 12803–12812.
47 Z. Yang, Z. Mao, X. Zhang, D. Ou, Y. Mu, Y. Zhang, C. Zhao, S. Liu, Z. Chi, J. Xu, Y.-C. Wu, P.-Y. Lu, A. Lien and M. R. Bryce, *Angew. Chem., Int. Ed.*, 2016, **55**, 2181–2185.
48 T. Lu and F. W. Chen, *J. Comput. Chem.*, 2012, **33**, 580–592.
49 S. Lower and M. El-Sayed, *Chem. Rev.*, 1966, **66**, 199–241.